NJC

Accepted Manuscript

This is an *Accepted Manuscript*, which has been through the Royal Society of Chemistry peer review process and has been accepted for publication.

Accepted Manuscripts are published online shortly after acceptance, before technical editing, formatting and proof reading. Using this free service, authors can make their results available to the community, in citable form, before we publish the edited article. We will replace this *Accepted Manuscript* with the edited and formatted *Advance Article* as soon as it is available.

You can find more information about *Accepted Manuscripts* in the Information for Authors.

Please note that technical editing may introduce minor changes to the text and/or graphics, which may alter content. The journal's standard Terms & Conditions and the Ethical guidelines still apply. In no event shall the Royal Society of Chemistry be held responsible for any errors or omissions in this *Accepted Manuscript* or any consequences arising from the use of any information it contains.

ROYAL SOCIETY OF CHEMISTRY

www.rsc.org/njc

SYNOPSIS TOC (Word Style "SN_Synopsis_TOC").

The ionic mechanistic model involving the heterolytic cleavage of B–H bond is slightly energetically favorable than the [2+2] addition mechanism for the high-valent oxo-molybdenum complex MoO_2Cl_2 activate the B–H bond.

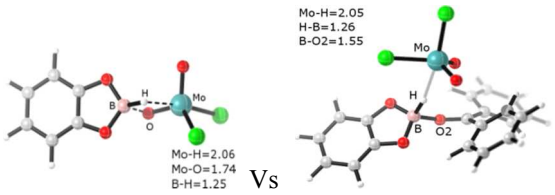

27.6 kcal/mol 26.9 kcal/mol

The **[2+2]** addition vs. the ionic mechanistic model

Journal Name

RSCPublishing

ARTICLE

Mechanistic insights into B-H bond activation with the high-valent oxo-molybdenum complex MoO_2Cl_2

Cite this: DOI: 10.1039/xoxxoooooox

Received ooth January 2012,
Accepted ooth January 2012

DOI: 10.1039/xoxxoooooox

www.rsc.org/

Liangfang Huang, Haiyan Wei*,

The B-H bond activation and the catalytic hydroboration of carbonyl compounds by the high-valent oxo-molybdenum complex MoO2Cl2 were theoretically investigated to determine the underlying mechanism. Our calculation results indicate an unique path – the ionic mechanistic pathway involving the heterolytic cleavage of the B–H bond is competing with the [2+2] addition pathway, which involves the B–H bond adding across one of the Mo=O bond. The rate-determining free energy barriers for the ionic mechanistic pathway are calculated to be 26.9 kcal/mol, 25.0 kcal/mol and 23.7 kcal/mol for diphenylketone, benzaldehyde and acetophenone, respectively. These values are energetically slightly favorable than the [2+2] addition mechanism by ~ 1- 3 kcal/mol. Furthermore, it is worth noting that the carbonyl compounds bearing the electron donation group will induce a better activity toward the ionic mechanistic pathway.

Introduction

The X–H (X=H, Si, B, C, etc) bond activation reactions are highly valuable because of their potentially important chemical transformations, which is employed in the functionalization of organic molecules, and is applied in the synthesis of new materials.[1-3] For many years, the low-valent transition metal complexes have been employed to activate such bonds. Detailed insights into the mechanism of the catalytic cycle revealed that most of these processes involve the oxidative addition of an X–H (X = H, Si, B, C, etc.) bond to the metal center.[4-5] However, since the hydrosilylation of carbonyl compounds catalyzed by the high-valent di-oxo-rhenium(V) complex $ReO_2I(PPh_3)_2$ was first reported in 2003 by Toste and co-workers,[6] the high-valent transition-metal complexes have became valuable catalysts for hydrogenation/hydrosilylation/hydroboration of various organic substrates. A series of oxo-molybdenum(VI)/rhenium(V)/ruthenium(VI) complexes (MoO_2Cl_2, $CpMoO_2Cl$, $Re(O)Cl_3(PPh_3)_2$, CH_3ReO_3, Re_2O_7, $HReO_4$, nitridoruthenium(VI), etc.)[7–10] are used as efficient catalysts for X–H (X=H, Si, B, C, etc.) bond activation reactions and the reduction of the functional groups (carbonyl groups, imines, esters, sulfoxides and pyridine-N-oxides, nitrile, etc.). These oxo-rhenium/molybdenum complexes have also been reported to reduce sulfoxides with boranes,[11] to afford the corresponding sulfides, as well as the P–H bond activation and the hydrophosphonylation of aldehydes[12] and imines,[13] to afford a-hydroxyphosphonates and a-aminophosphonates.

On the basis of the experimental findings, Toste and co-workers proposed a [2+2] addition mechanism (Scheme 1) to account for the catalytic hydrosilylation reaction mediated by the di-oxo rhenium(V) complex $ReO_2I(PPh_3)_2$.[7a] In the proposed mechanism, the activation of Si–H bond through its addition across one of the Re=O bonds in a [2+2] manner, which results the addition of silyl hydride to the metal center and of the cation (SiR_3^+) to the oxide ligand, was considered the first step. The rhenium hydrido intermediate $ReO(OSiR_3)(H)(I)(PPh_3)_2$ is then postulated as the activate intermediate in the subsequent reduction of carbonyl substrates. This occurs via the coordination of carbonyls to the rhenium center, followed by their migratory insertion into the M−H bond. The last step of the catalytic cycle is a retro-[2 + 2] addition that corresponds to the alkoxide group attacking the silyloxium group to produce silyl ether and regenerate the catalyst. Later, the [2+2] addition mechanism was explored computationally by Wu and co-workers,[13] and confirmed to be the preferred reaction pathway. Their density functional theory (DFT) results indicated that the activation of the Si–H bond is the rate-determining step in the carbonyl hydrosilylation reaction catalyzed by the di-oxo-rhenium(V) complex $ReO_2I(PPh_3)_2$. Typically, the binding and cleavage of X−H (X = H, Si, B) bonds have close resemblance to each other. The [2+2] addition mechanism was likewise suggested in the hydrogenation and hydroboration of double and triple bonds, like, for the activation of B−H bond of borane by high-valent di-oxo-molybdenum complex.[14]

Scheme 1 Proposed [2+2] addition mechanism for the hydrosilylation of carbonyl compounds by di-oxo-rhenium(V) complex $ReO_2I(PPh_3)_2$.

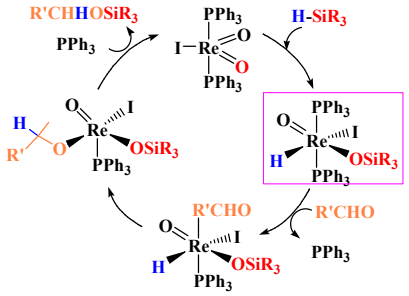

The role of high-valent transition metal complexes as catalysts for oxidative reactions has thus been totally reversed and opens an entirely new area of catalysis for these complexes.[15] However, the underlying mechanism of the reduction reaction catalyzed by these high-valent transition metal complexes has remained largely unexplored theoretically.[16] Our group is interested in exploring the reaction mechanism of the high-valent transition metal complexes activating the X−H bond and catalyzing the reduction reaction.[17] We herein report the reaction mechanism of the hydroboration (HBcat = 1,3,2-benzodioxaborolane) of aldehyde/ketone catalyzed by the high-valent di-oxo-molybdenum(VI) complex MoO_2Cl_2 (scheme 2) by theoretical calculations.[18,19] Although the B–H activation of boranes with the high-valent oxo-molybdenum complex was proposed to involve of [2+2] addition mechanism, the evidence in support of an intermediate with the Mo–H bond from experimental observation remains elusive.[19] Through detailed investigation, our results suggested that an unique path – the ionic mechanistic pathway involving the heterolytic cleavage of the B–H bond operates in the activation of B–H bond by the high-valent oxo-molybdenum complex MoO_2Cl_2. And the ionic mechanistic pathway is slightly favorable than the previously proposed [2+2] addition mechanism.

Scheme 2 Catalytic reduction of aldehyde/ketone mediated by MoO_2Cl_2/HBcat system in this study.

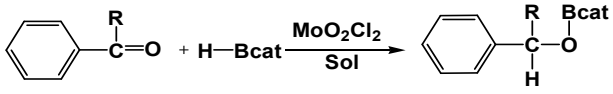

The ionic mechanistic pathway has been proposed to account for the catalytic hydrosilylation of carbonyl compounds by tris(pentafluorophenyl)borane reported by Piers,[20] and the hydrosilylation of epoxides, amides, aldehyde/ketone, and ester, as well as the reduction of alky halides by a cationic iridium catalyst reported by Brookhart,[21] as well as the hydrosilylation of carbonyl compounds by the high-valent oxo-rhenium(V) complex $Re(O)Cl_3(PPh_3)_2$[8d]. As shown in Scheme 3, the ionic mechanistic catalytic cycle is initiated by a carbonyl substrate nucleophilic attack on the η^1-silane metal/borane adduct, which results in the heterolytic cleavage of the Si–H bond, prompts transfer of the R_3Si^+ ion to carbonyl compounds, generates the silylated aldehyde/ketone. Then the hydride on the metal/borane center transfers to the activated silylcarbenium ion to furnish the reduction reaction. In the ionic mechanistic model, the mechanistic requirement for the migratory insertion of unsaturated carbonyl species is removed, thus widening the range of transition metals that can be used.[22-24] However, to the best of our knowledge, there are relatively few theoretical investigations studying a reaction favoring the ionic mechanistic pathway catalyzed by the transition-metal complexes,[25] especially by the neutral transition-metal complexes. The present study provides a greater understanding of the activation of B–H bond by the high-valent di-oxo-molybdenum complexes.

Scheme 3 Proposed ionic mechanistic pathway for hydrosilylation of carbonyl compounds by tris(pentafluorophenyl)borane, cationic iridium catalyst, and mono-oxo-rhenium(V) complex.

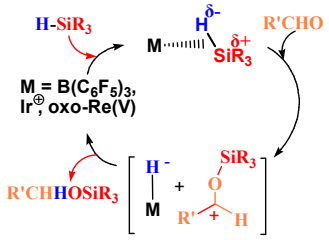

Computational Methods

All molecular geometries of the model complexes were optimized using hybrid meta exchange-correlation M06 methods,[26] which include medium-range correlation as implemented in Gaussian 09.[27] The effective core potentials (ECPs) of Hay and Wadt with double-ζ valence basis sets (LanL2DZ)[28] were used to describe the Mo metals. In addition, polarization functions were added for Mo (ζ_f = 1.043).[29-30] The 6-311g(d,p) basis set was used for all other atoms, such as B, C, H, O, and Cl. All geometric optimizations were performed under solvent conditions using the SMD solvation model with THF as the solvent using tight convergence criteria and pruned ultrafine grids (The SMD model is an IEFPCM calculation with radii and non-electrostatic terms for Truhlar and coworkers' SMD solvation model[31]). Frequency calculations at the same level of theory were carried out to verify all stationary points as minima (zero imaginary frequency) and transition states (one imaginary frequency). The transition states found were further confirmed by calculating intrinsic reaction coordinates routes toward the corresponding minima and reoptimization from the final phase of IRC paths to reach each minimum.

The final Gibbs energies values for ΔG reported in this paper are relative Gibbs free energies calculated at 298 K in solution, by carrying out a single-point calculation using the larger basis set of quintuple zeta set with extra polarization basis sets (cc-QVZP) for molybdenum and 6-311++G (2d,p) for the rest of atoms.[32] All the geometries are displayed using the software of CYLview.[33]

Results and Discussion

[2+2] addition mechanism: Homolytic activation is usually proposed to involve the oxidative addition, thus requiring the metal center to have an oxidation state with two units higher. However, this is not available for the d^0 Mo(VI) derivatives (MoO_2Cl_2, here). Instead, an alternative [2+2] addition mechanism in which the X–H (X=Si, B) bond adds across one of Mo=O bonds is proposed to account for hydrosilylation/hydroboration of organic substrates. Thus the multiply bounded oxido ligand plays an important role in assisting the activation of the X–H bond.

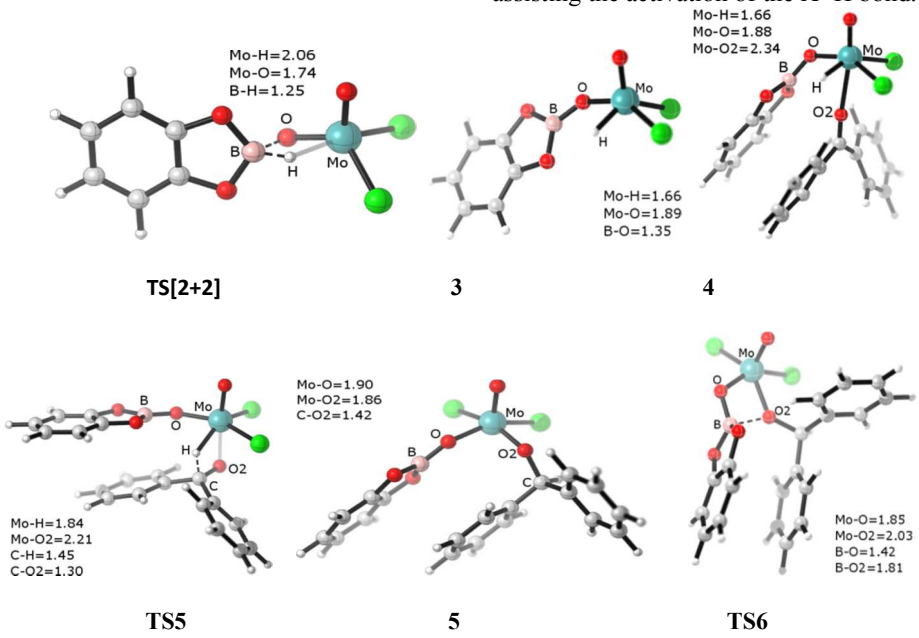

Figure 1. Optimized structures of the transition states of the transition states **TS[2+2]**, **TS5** and **TS6** and intermediates **3**, **4** and **5** along the [2+2] addition pathway for catalytic reduction of ketone by MoO_2Cl_2/HBcat system. Bond distances are shown in Å.

As shown in Figure 1, the optimized structure of the transition state **TS[2 + 2]** has a four-membered cyclic (O···B···H···Mo) ring, representing the catecholborane (HBcat) hydrogen abstracted by the molybdenum center (*d*(Mo···H) = 2.06 Å) and the Bcat group to form a bond with the multiply bound oxido ligand (*d*(Mo···O) = 1.74 Å). The transition state **TS[2 + 2]** leads to the hydride intermediate **3**, in which the hydride is coordinated to the molybdenum center, with a normal Mo–H bond of 1.66 Å. This [2+2] addition step is associated with an activation free energy barrier of 27.6 kcal/mol relative to catalyst MoO_2Cl_2 and HBcat. The hydride intermediate **3** is 3.6 kcal/mol higher than the sum of isolated reagents (MoO_2Cl_2 + HBcat). Afterward, the ketone molecule (here diphenylketone) coordinating weakly to the molybdenum center, forms an η^1-ketone intermediate **4** (Figure 1). The coordination geometry around the molybdenum atom in **4** can be viewed as a distorted octahedron with diphenylketone residing *trans* to the multiply bound oxido ligand, with a long Mo–O2 distance of 2.34 Å. The formation of **4**, MoO(H)(OBcat)(Ph_2CO)Cl_2, is endergonic by 3.9 kcal/mol from catalyst MoO_2Cl_2, HBcat and diphenylketone.

To proceed, the η^1-coordinated diphenylketone inserts into the Mo–H bond () to form an alkoxide complex. This migratory insertion occurs as a concerted process (by **TS5**, Figure 1) through a four-member ring consisting of Mo–H and C=O2 bonds. In the optimized structure of the transition state **TS5**, the Mo–O2 distance decreases to 2.21 Å, whereas the Mo–H distance considerably lengthens to 1.84 Å, together with the C=O bond is elongated to be halfway between a double and a single bond (1.30 Å). **TS5** is associated with an overall barrier of 26.1 kcal/mol higher than the reactants (**1** + diphenylketone + HBcat). The formation of the insertion product, i.e., alkoxide intermediate **5**, MoO(OBcat)($OCHPh_2$)Cl_2 is largely exergonic by 13.5 kcal/mol from catalyst MoO_2Cl_2, HBcat and diphenylketone.

To complete the catalytic cycle, the forward reaction involves a retro-[2+2] addition, which represents the transfer of the boryl group to the alkoxy oxygen. The corresponding transition state **TS6** (Figure 1), comprised of a four-member ring, in which the B–O2 distance decreases to 1.81 Å and the B–O bond is elongated to 1.42 Å. The activation barrier of the retro-[2+2] addition is 16.3 kcal/mol above the alkoxide intermediate **5**. By separating from the catalyst, the product $Ph_2CHOBcat$ is formed, and the catalyst MoO_2Cl_2 is regenerated.

Journal Name RSCPublishing

ARTICLE

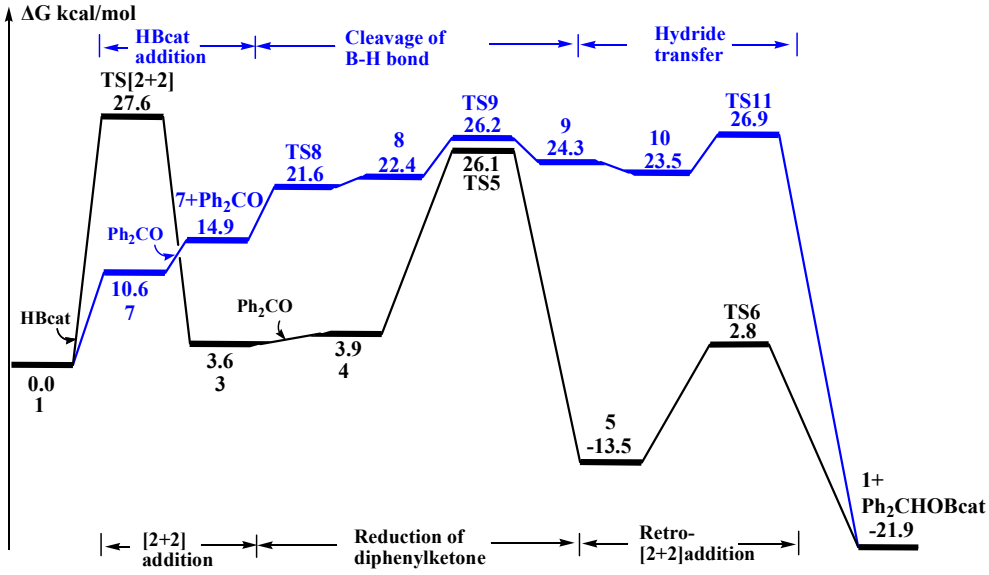

Figure 2. Schematic free-energy surface for MoO_2Cl_2 mediated the hydroboration of diphenylketone through the [2+2] addition pathway (black) and the ionic mechanistic pathway (blue).

Figure 2 summarizes the calculated free energies for the high-valent di-oxo-molybdenum complex MoO_2Cl_2-catalyzed hydroboration of diphenylketone via the [2+2] addition pathway (black). The calculated energies of the [2+2] addition transition state involving the B–H bond adding across one of the Mo=O bonds to form the molybdenum hydride intermediate is 27.6 kcal/mol. The following steps for the generating molybdenum hydride intermediate **3** acting as an active species to reduce ketone is associated with an activation free energy of 22.4 kcal/mol (**TS5** above **4**), and the retro-[2+2] addition is associated with an activation free energy of 17.3 kcal/mol (**TS6** above **5**). Thus, it is evident that the [2+2] addition step is the turnover-limiting step in the [2+2] addition pathway.

Ionic mechanistic pathway: The ionic mechanistic catalytic cycle featured by the organic substrates nucleophilic attacking the borane metal adduct. This attack results in the heterolytic cleavage of the B–H bond and generation of anion pair comprised of a boryl carbenium ion paired with an anionic molybdenum hydride, $[MoO_2Cl_2(H)]^-[catBOCR'R'']^+$. Then transferring the hydride from the metal center to the boryl carbenium ion yields the boryl ether product. For such a reaction pathway, the coordination of the organic substrate to the metal center is not needed. Figure 2 (blue) illustrates the ionic mechanistic pathway for the di-oxo-molybdenum complex MoO_2Cl_2 catalyzed the hydroboration of diphenylketone, together with the energetic results. The optimized geometries for the species considered in the ionic mechanistic pathway are depicted in Figure 3. The ionic mechanistic pathway is initiated with borane coordinated to the molybdenum center. A borane molybdenum complex was formed, **7** displaying a significantly long Mo···H distance (3.24 Å) and a normal B−H bond length (1.17 Å). These features indicated that the η^1-bonded borane molybdenum complex is a loose bonded η^1-borane structure. Complex **7** is 10.6 kcal/mol above the separation of MoO_2Cl_2 and a free HBcat.

The next step is for diphenylketone molecule approaching the η^1-borane complex **7**. Initially, a loosely bound adduct **7+Ph$_2$CO** forms. In the optimized structure of adduct **7+Ph$_2$CO** (Figure 3), the η^1-borane hydrogen moves closer to molybdenum center, at a Mo···H distance of 2.94 Å. While the isolated structures of η^1-borane complex **7** and diphenylketone are barely perturbed, exhibiting a significantly long B···O2 (diphenylketone) distance of 2.54 Å. The formation of adduct **7+Ph$_2$CO** is endergonic by 14.9 kcal/mol from catalyst MoO_2Cl_2, HBcat and diphenylketone.

Then, the attacks of nucleophilic diphenylketone to the boron center results in cleaving of the B–H bond. For this process, as we take either H···B or B···O2 (diphenylketone) separation as the reaction coordinate, a consecutive process (two steps) representing the heterolytic cleavage of the B−H bond could be identified. Analyses of these two steps are described in the following.

Journal Name RSCPublishing

ARTICLE

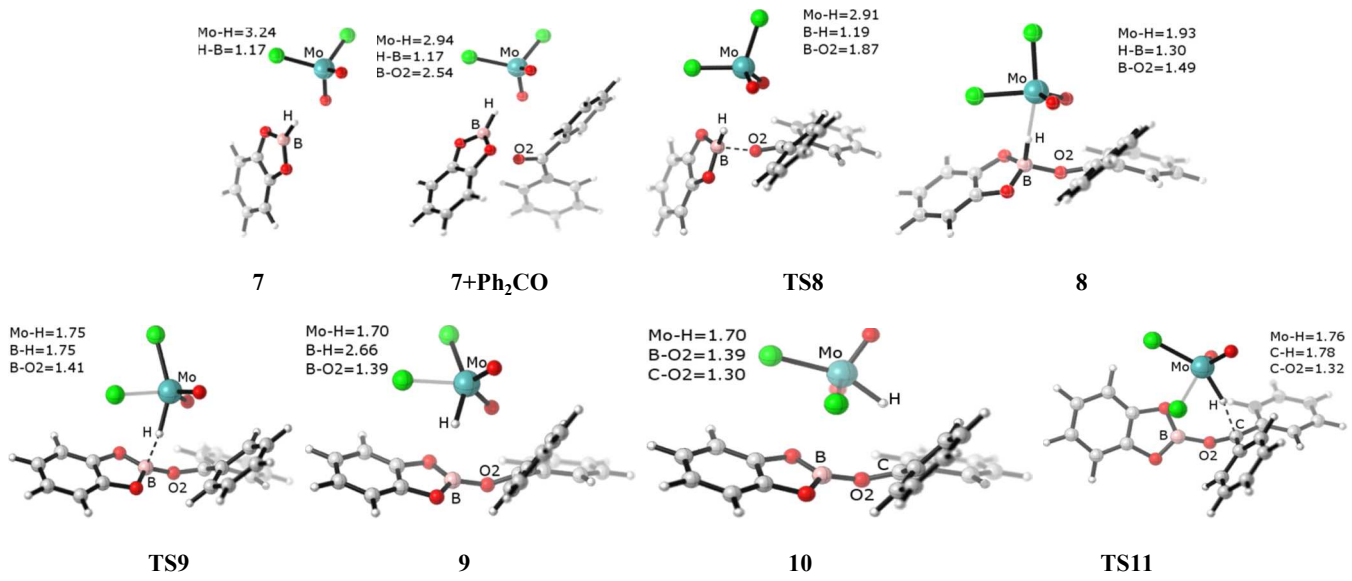

Figure 3. Optimized structures of the transition states **TS8**, **TS9**, and **TS11** and intermediates **7**, **7+Ph$_2$CO**, **8**, **9** and **10** along the ionic mechanistic pathway for catalytic reduction of diphenylketone by MoO_2Cl_2/HBcat system. Bond distances are shown in Å.

The first transition state **TS8** corresponds to approach of the diphenylketone oxygen atom to the boron atom, which is accompanied by elongation of the B−H bond, with hydrogen moving toward the molybdenum center. In the optimized structure of **TS8** (Figure 3), the B–H bond is lengthened to 1.19 Å (compared with 1.17 Å in HBcat). The Mo···H separation is shortened to 2.91 Å, which is 0.03 Å shorter than the adduct **7+Ph$_2$CO**. The B···O2 separation is shortened to 1.87 Å (compared with 2.54 Å in the adduct **7+Ph$_2$CO**). The vibrational motion associated with the imaginary frequency in **TS8** represents the diphenylketone oxygen atom coupling with the boron center. The free energy barrier in **TS8** is 21.6 kcal/mol.

The transition state **TS8** leads to intermediate **8** located in a shallow minimum.[34] The intermediate **8** describes half of the process of B–H bond cleavage, with the B−H bond elongated to 1.30 Å. It also describes half of the formation of B−O2 (**Ph$_2$CO**) bond, withthe borane–oxygen distance shortened to 1.49 Å from 2.54 Å (in **7+Ph$_2$CO)**, and half of the formation of Mo−H bond, with molybdenum-hydride distance shortened to 1.93 Å from 2.94 Å (in **7+Ph$_2$CO)**. The geometry around the boron atom in **8** can be described as a tetrahedron structure with the boron atom located at the center, which exhibits a *syn* S_N2-B reaction mode. The carbonyl oxygen of diphenylketone adds "front-side" to the boron in adduct **7** and promotes the heterolytic cleavage of the B−H bond. The newly formed B−O2 bond lying resides *syn* to the partially broken B–H bond, with the Mo−H−B angle of 150.8°and the O2−B−H angle of 104.8°.

Proceeding from intermediate **8**, the heterolytic cleavage of B−H bond occurs. The corresponding transition state is located as **TS9**. In the optimized structure of **TS9**, the B–H bond is partially broken with distance of 1.75 Å. The Mo–H bond is formed, *d*(Mo–H) = 1.75 Å. And the B–O2 bond is shortened to 1.41 Å. The vibrational motion associated with the imaginary frequency in **TS9** represents the borane hydrogen transferred to the molybdenum center, and the boryl ion (Bcat) couples to diphenylketone. The heterolytic cleavage of B−H bond by passing **TS9** is calculated to have an energy barrier of 26.2 kcal/mol within the catalytic cycle. Passing **TS9**, the cleavage of the B−H bond forms an intermediate **9**, comprised of an molybdenum hydride anion and borylated ketone ion. In the optimized structure of intermediate **9**, the two moieties $[MoO_2Cl_2H]^-$ and $[Ph_2COBcat]^+$ are largely separated by a long distance of 2.66 Å (B···H separation). Our analysis shows that the intermediate **9** is 1.9 kcal/mol lower than the transition state **TS9**.

Along the process: **7+Ph$_2$CO→TS8→8→TS9→9**, the diphenylketone molecule approaches the borane center with the *d*(O2··B) decreasing in the order 2.54 Å → 1.87 Å → 1.49 Å → 1.41 Å → 1.39 Å, which simultaneously prompts the stretching of the B−H bond by 1.17 Å → 1.19 Å → 1.30 Å → 1.75 Å→ 2.66 Å, respectively. At the same time, the borane hydrogen progressively binds to the molybdenum center as the Mo···H distance decreases by 2.94 Å → 2.91 Å → 1.93 Å → 1.75 Å→ 1.70 Å. NBO charge analysis along this process revealed that the electron density from the borane hydrogen

progressively drains toward the molybdenum center. The calculated NBO negative charge on the borane hydrogen decreases by (-0.14*e*, -0.15*e*) → (-0.05*e*, -0.02*e*) along **TS8→8→TS9→9**. However, the NBO charge on the molybdenum becomes less positively charged, i.e. (1.02*e*, 1.03*e*) → 0.94*e* → 0.81*e* → 0.78*e* along the transition**.** Conversely, the NBO charge on the borane reversed, which becomes more positively charged, along 0.99*e* →0.96*e* → 1.09 *e* →1.28*e* →1.31*e* along the path.

To complete the catalytic cycle, from the intermediate **9**, the hydride attached to the molybdenum center transfers to the carbon atom of borylated ketone $[Ph_2COBcat]^+$, to produce the boryl ether product. Initially, another conformation of the ion pair, **10** forms (Figure 3), by repositioning the two moieties of molybdenum hydride anion $[Mo(O)_2(Cl)_2H]^-$ and the borylated carbenium ion $[Ph_2COBcat]^+$. In the optimized structure of the intermediate **10**, the Mo−H bond points toward the carbon atom of the borylated carbenium ion, with the angle Mo···H···C (C=O) being 142.2º, whereas the Mo−H bond assumes the perpendicular position to the boron atom of the borylated carbenium ion in **9.** From **10**, the borylated carbenium ion easily abstracts the hydride bonded at the molybdenum center. This process occurs through the transition state **TS11**. In the optimized structure of **TS11**, the hydride moves to the carbon atom of the diphenylketone, with the Mo···H bond being elongated to 1.76 Å, and the C···H bond is shortened to 1.78 Å. And this process is associated with a low activation free energy barrier (3.4 kcal/mol, **TS11** above **10**). It is worth noting that, once the intermediate **9** is generated, the ion pair can readily undergo isomerization (ΔG(**9 →10**) = -0.8 kcal/mol), as well as undergo the hydride transfer reaction from the molybdenum to the borylated carbenium ion via **TS11** (ΔG(**10 →TS11**)= 3.4 kcal/mol). Furthermore, the driving force for the hydride transfer reaction is large by 45.4 kcal/mol, (**10**→MoO_2Cl_2+$Ph_2CHOBcat$), which likely originates from the strong electrostatic attraction between the hydride on the molybdenum and the borylcarbonium carbon atom.

The calculated ionic mechanistic pathway derived from our DFT calculations for reducing diphenylketone using the MoO_2Cl_2/HBcat system, shown in Figure 2(blue), can be divided into three steps: (1) the addition of borane to the metal center, **1**→ **7**; (2) the heterolytic cleavage of the B–H bond through the nucleophilic attack of diphenylketone, **7+Ph_2CO→TS8→8→TS9→9**, to generates the ion pair comprised of the molybdenum hydride anion and borylated ketone ion; (3) the hydride transfers to the carbonyl carbon , and regenerates the catalyst, **10→TS11→1**. The heterolytic cleavage of the B–H bond (**TS9**) and the hydride transfer step (**TS11**) represent the highest activation barrier along the ionic mechanistic pathway, with the overall activation free energies of 26.2 and 26.9 kcal/mol, respectively.

With these preliminary results in hand, a range of carbonyl compounds, including benzaldehyde, acetophenone and p-methoxybenzaldehyde, p-methoxybenzophenone wereinvestigated. Notably, our calculations indicated that the steric effect is negligible on the activation free energies of the rate-determing step along the ionic mechanistic pathway. The activation free energies of the rate-determing step are 21.5 kcal/mol (**TS9**), 25.0 kcal/mol (**TS11**) with benzaldehyde; 23.7 kcal/mol (**TS9**), 23.5 kcal/mol (**TS11**) with acetophenone, respectively, which is about 2~3 kcal/mol lower than that with diphenylketone (26.9 kcal/mol, **TS11**). Furthermore, it is worth noting that organic substrates bearing electron donating group show better activity for the ionic mechanistic pathway. With p-methoxybenzaldehyde, the activation free energy associated with the heterolytic cleavage of B–H bond (**TS9**) is lowered to be 19.5 kcal/mol (compared to 21.5 kcal/mol of benzaldehyde). With p-methoxybenzophenone, the activation free energies associated with the heterolytic cleavage of B–H bond step (**TS9**) is calculated to be 22.3 kcal/mol. This can be ascribed to the cationic boryl center being stabilized by the electron donation group on phenyl group in the transition state structure.

Therefore, for the high-valent di-oxo-molybdenum complex MoO_2Cl_2-catalyzed hydroboration, the [2+2] addition pathway discussed (Figure 2, black) is competing with the ionic mechanistic pathway The activation energy barrier of the [2+2] addition pathway (~27.6 kcal/mol) is slightly higher than that of the ionic mechanistic pathway (26.9 kcal/mol (diphenylketone), 25.0 kcal/mol (benzaldehyde), 23.7 kcal/mol (acetophenone). These results indicate that both pathways operate in the hydroboration of diphenylketone by the high-valent di-oxo-molybdenum complex MoO_2Cl_2. Moreover, in a particular system addressed, the ionic mechanistic pathway and the [2+2] addition pathway should be competitive. Furthermore, small changes in the system, particular in the organic substrates may play a major role and favor one of the other two alternatives.

Conclusions

In summary, our calculation results show that the reactivity of the high-valent di-oxo-molybdenum(VI) MoO_2Cl_2 for activating the B–H bond are different from activating the Si–H bond with the carbonyl compounds. Through a detailed investigation, we showed that the high-valent di-oxo-molybdenum(VI) complex MoO_2Cl_2-catalyzed hydroboration of carbonyl compounds proceeds via two competing reaction pathways: the ionic mechanistic pathway and the [2+2] addition pathway. Furthermore, the ionic mechanistic pathway, in which the carbonyl compounds carry out a nucleophilic anti attack at the molybdenum borane adduct, to prompt the heterolytic cleavage of the B−H bond is slightly energetic favorable than the [2+2] addition pathway by ~2-3 kcal/mol.

There are two clear differences between the ionic mechanism and the [2+2] addition mechanism, which center on whether the multiple bounded oxido ligand participates in the reaction and whether the reduced species is initially coordinated to the metal. Moreover, for the reaction proceeding via the ionic mechanistic pathway, the coordination of the organic substrate to the metal center, and subsequent insertion into the TM–H bond, are not needed, thus broadening the range of transition metals that can be used. Our calculations provide useful insights for the fundamental understanding of the activation of

the X–H bond and the reduction reaction mediated by those high-valent transition-metal complexes. Further studies may ultimately lead to the design of more efficient catalysts that favor the ionic mechanism based on the mechanistic understanding gained in this study.

Acknowledgements

We acknowledge the support of the National Natural Science Foundation of China (No. 21103093), the Jiangsu Province Science and Technology Natural Science Project (No. BK2011780), the Chair Professor of Jiangsu Province to Start Funds, a Project Funded by the Priority Academic Program Development of Jiangsu Higher Education Institutions, and a Project Funded by Jiangsu Collaborative Innovation Center of Biomedical Functional Materials. We also thank the Shanghai Supercomputer Center and the Nanjing University HPCC for their technical support.

Notes and references

[a]Jiangsu Key Laboratory of Biofunctional Materials, School of Chemistry and Materials Science, Jiangsu Provincial Key Laboratory for NSLSCS, Nanjing Normal University, Nanjing 210097, China

† Electronic Supplementary Information (ESI) available: [Complete Ref. 27, comparison of different basis set levels, additional results not shown in the text, and Cartesian coordinates of all optimized structures discussed in the paper.. See DOI: 10.1039/b000000x/

1 (a) G. J. Kubas, *Metal Dihydrogen and σ-Bond Complexes: Structure, Theory and Reactivity*, Kluwer, New York, **2001**. (b) G. J. Kubas, *Chem. Rev.* **2007**, *107*, 4152. (c) J. A. Labinger, J. E. Bercaw, *Nature*. **2002**, *417*, 507. (d) G. Alcaraz, S. Sabo-Etienne, *Angew. Chem., Int. Ed.* **2010**, *49*, 7170.

2 (a) A. J. Cowan, M. W. George, *Coord. Chem. Rev*. **2008**, *252*, 2504. (b) S. Sabo-Etienne, B. Chaudret, *Coord. Chem. Rev*. **2008**, *252*, 2395. (c) J. Y. Corey, *Chem. Rev*. **2011**, *111*, 863. (d) C. Hall, R. N. Perutz, *Chem. Rev*. **1996**, *96*, 3125.

3 (a) A. Staubitz, A. P. M. Robertson, I. Manners, *Chem. Rev.* **2010**, *110*, 4079. (b) J. E. Bercaw, J. A. Labinger, *Proc. Natl. Acad. Sci. U.S.A*. **2007**, *104*, 6899. (c) W. H. Bernskoetter, C. K. Schauer, K. I. Goldberg, M. Brookhart, *Science*. **2009**, *326*, 553.

4 (a) I. A. I. Mkhalid, J. H. Barnard, T. B. Marder, J. M. Murphy, J. F. Hartwig, *Chem. Rev*. **2010**, *110*, 890. (b) V. Pons. R. T. Baker, *Angew. Chem., Int. Ed*. **2008**, *47*, 9600. (c) A. Staubitz, A. P. M. Robertson, M. E. Sloan, I. Manners, *Chem. Rev*. **2010**, *110*, 4023. (d) J. R. Fulton, A. W. Holland, D. J. Fox, R. G. Bergman, *Acc. Chem. Res*. **2002**, *35*, 44. (e) T. B. Gunnoe. *Eur. J. Inorg. Chem*. **2007**, 1185. (f) H. Braunschweig, R. D. Dewhurst, A. Schneider, *Chem. Rev*. **2010**, *110*, 3924. (h) K. Burgess, M. J. Ohlmeyer, *Chem. Rev*. **1991**, *91*, 1179.

5 (a) A. J. Chalk, J. F. Harrod, *J. Am. Chem. Soc*. **1965**, *87*, 16. (b) I. Ojima, M. Nihonyanagi, Y. Nagai, *J. Chem. Soc, Chem. Commun*. **1972**, 938. (c) I. Ojima, M. Nihonyanagi, T. Kogure, M. Kumagai, S. Horiuchi, K. Nakatsugawa, Y. Nagai, *J. Organomet. Chem*. **1975**, *94*, 449. (d) M. Kobayashi, T. Koyama, K. Ogura, S. Seto, F. J. Ritter, I. E. M. Brueggemann-Rotgans, *J. Am. Chem. Soc*. **1980**, *102*, 6602. (e) M. F. Semmelhack, R. N. Misra, *J. Org. Chem*. **1982**, *47*, 2469. (f) I. Ojima, T. Kogure, *Organometallics*. **1982**, *1*, 1390.

6 J. J. Kennedy-Smith, K. A. Nolin, H. P. Gunterman, F. D. Toste, *J. Am. Chem. Soc*. **2003**, *125*, 4056.

7 (a) K. A. Nolin, J. R. Krumper, M. D. Pluth, R. G. Bergman, F. D. Toste, *J. Am. Chem. Soc*. **2007**, *129*, 14684. (b) B. D. Sherry, A. T. Radosevich, F. D. Toste, *J. Am. Chem. Soc.* **2003**, *125*, 6076. (c) B. D. Sherry, R. N. Loy, F. D. Toste, *J. Am. Chem. Soc*. **2004**, *126*, 4510. (d) M. R. Luzung, F. D. Toste, *J. Am. Chem. Soc*. **2003**, *125*, 15760. (e) J. J. Kennedy-Smith, L. A. Young, F. D. Toste, *Org. Lett*. **2004**, *6*, 1325. (f) K. A. Nolin, R. W. Ahn, F. D. Toste, *J. Am. Chem. Soc*. **2005**, *127*, 12462. (g) R. V. Ohri, A. T. Radosevich, K. J. Hrovat, C. Musich, D. Huang, T. R. Holman, F. D. Toste, *Org. Lett.* **2005**, *7*, 2501. (h) A. T. Radosevich, C. Musich, F. D. Toste, *J. Am. Chem. Soc.* **2005**, *127*, 1090. (i) K. A. Nolin, R. W. Ahn, F. D. Toste, *J. Am. Chem. Soc*. **2005**, *127*, 17168. (j) A. Blanc, F. D. Toste, *Angew. Chem., Int. Ed*. **2006**, *45*, 2096.

8 (a) E. A. Ison, E. R. Trivedi, R. A. Corbin, M. M. Abu-Omar, *J. Am. Chem. Soc*. **2005**, *127*, 15374. (b) G. Du, G. M. M. Abu-Omar, *Organometallics*. **2006***, 25*, 4920. (c) E. A. Ison, E. A. Corbin, M. M. Abu-Omar, *J. Am. Chem. Soc.* **2005**, *127*, 11938. (d) G. Du, P. E. Fanwick, M. M. Abu-Omar, *J. Am. Chem. Soc*. **2007**, *129*, 5180. (e) E. A. Ison, J. E. Cessarich, G. Du, P. E. Fanwick, M. M. Abu-Omar, *Inorg. Chem*. **2006**, *45*, 2385. (f) R. A. Corbin. E. A. Ison, M. M. Abu-Omar, *Dalton Trans*. **2009**, 2850. (g) G. S. Owens, J. Aries, M. M. Abu-Omar, *Catal. Today*. **2000**, *55*, 317.

9 (a) B. Royo, C. C. Romão, *J. Mol. Catal. A: Chem*. **2005**, *236*, 107. (b) A. C. Fernandes, R. Fernandes, C. C. Romão, B. Royo, *Chem. Commun.* **2005**, 213. (c) A. C. Fernandes, C. C. Romão, *Tetrahedron Lett*. **2005**, *46*, 8881. (d) A. C. Fernandes, C. C. Romão, *Tetrahedron* **2006**, *62,* 9650. (e) A. C. Fernandes, C. C. Romão, *J. Mol. Catal. A: Chem*. **2006**, *253*, 96. (f) A. C. Fernandes, J. A. Fernandes, F. A. Almeida, C. C. Romão, *Dalton Trans*. **2008**, 6686. (g) R. G. Noronha, P. J. Costa, C. C. Romão, M. J. Calhorada. A. C. Fernandes, *Organometallics*. **2009**, *28*, 6206.

10 (a) D. V. Gutsulyak, L. G. Kuzmina, J. A. K. Howard, S. F. Vyboishchikov, G. I. Nikonov, *J. Am. Chem. Soc*. **2008**, *130*, 3732. (b) D. V. Gutsulyak, L. G. Kuzmina, J. A. K. Howard, S. F. Vyboishchikov, G. I. Nikonov, *Organometallics*. **2009***, 28*, 2655. (c) A. Y. Khalimon, O. G. Shirobokov, E. Peterson, R. Simionescu, L. G. Kuzmina, G. I. Nikonov, *Inorg. Chem*. **2012**, *51*, 4300. (d) O. G. Shirobokov, R. Simionescu, L. G. Kuzmina, G. I. Nikonov, *Chem. Commun.* **2010,** *46*, 7831. (e) E. Peterson, A. Y. Khalimon, R. Simionescu, L. G. Kuzmina, J. A. K. Howard, G. I. Nikonov, *J. Am. Chem. Soc*. **2009**, *131*, 908. (f) S. Abbina, S. Bian, C. Oian, G. D. Du, *ACS Catal*. **2013**, *3*. 678.

11 (a) S. C. A. Sousa, I. Cabrita, A. C. Fernandes, *Chem. Soc. Rev*. **2012**, *41*, 5641. (b) I. Cabrita, S. C. A. Sousa, A. C. Fernandes, *Tetrahedron Lett.* **2010**, *51*, 6132. (c) A. C. Fernandes, C. C. Romão, *Tetrahedron Lett*. **2007**, *48*, 9176. (d) A. C. Fernandes, J. A. Fernandes, C. C. Romão, L. F. Veiros, M. J. Calhorda, *Organometallics*. **2010**, *29*, 5517.

12 (a) R. G. Noronha.; P. J. Costa.; C. C. Romão.; M. J. Calhorda.; A. C. Fernandes. *Organometallics. 2009*, **28,** 6*206.* (b) R. G. Noronha.; C. C. Romão.; A. C. Fernandes. *Catal. Commun*. **2011**, 12, 337.

13 L. W. Chu*ng*, *H. G. Lee, Z. L*in**, Y.** *D.* Wu. *J. Org. Chem*. **2006**, *71*, 6000.

14 M. J. Calhorda, P. J. Costa, *Dalton Trans*. **2009**, 8155**.**

15 W. R. Thiel, *Angew. Chem., Int. Ed*. **2003**, *42*, 5390.

16 (a) P. J. Costa, C. *C. Romão,* **A. C.** F*e*rnandes, B. Roya, P. M. Reis, M. J. Calhorda, *Chem. Eur. J.* **2007***, 13,* 3934. (b) *D. Markus,* T. Str*a*ssner, *Inorg. Chem*. **2007**, *46*, 10850.

17 W. W. Wang, P, Gu, Y. O. Wang, H**.** Y. Wei. *Organometallics*. **2014**, *33*, 847.

18 R. G. Parr, W. Yang, Density Functional Theory of Atoms and Molecules; O**xford** U**niver**sity Press: New York, **1989**.

19 P. M. Reis, C. C. Romão, B. Royo, *Dalton Trans*. **2006**, 1842.

20 (a) D. J. Parks, J. M. Blackwell, W. E. Piers, *J. Org. Chem*. **2000**, *65,* 3090. (b) D. J. Parks, W. E. Piers, *J. Am. Chem. Soc.* **1996**, *118*, 9440. (c) D. J. Parks, W. E. Piers, M. Parvez, R. Atencio, M. J. Zaworotko, *Organometallics.* **1998**, *17*, 1369. (d) J. M. Blackwell, E. R. Sonmor, T. Scoccitti, W. E. Piers, *Org. Lett.* **2000**, *2,* 3921. (e) A. Berkefeld, W. E. Piers, M. Parvez, *J. Am. Chem. Soc*. **2010**, *132,* 10660.

21 (a) V. K. Dioumaev, R. M. Bullock, *Nuture.* **2003**, *424*, 530. (b) R. M. Bullock, M. H. Voges, *J. Am. Chem. Soc*. **2000**, *122*, 12594. (c) W. H. Bernskoetter, S. K. Hanson, R. M. Brookhart, *J. Am. Chem. Soc*. **2009**, *131*, 8603. (d) S. Park, M. Brookhart, *J. Am. Chem. Soc*. **2012**, *134*, 640. (e) M. Findlater, W. H. Bernskoetter, M. Brookhart, *J. Am. Chem. Soc*. **2010**, *132*, 4534. (f) G. C. Welch, D. W. Stephan, *J. Am. Chem. Soc.* **2007**, *129*, 1880.

22 (a) A. Comas-Vives, G. Ujaque, *J. Am. Chem. Soc.* **2013**, *135*, 1295. (b) R. H. Morris, *Coord. Chem. Rev*. **2004**, *248*, 2201.

23 (a) C. A. Sandoval, T. Ohkuma, K. Muniz, R. Noyori, *J. Am. Chem. Soc.* **2003**, *125*, 13490. (b) K. Abdur-Rashid, S. E. Clapham, A. Hadzovic, J. N. Harvey, A. J. Lough, R. H. Morris, *J. Am. Chem. Soc*. **2002**, *124*, 15104.

24 (a) C. P. Casey, G. A. Bikzhanova, Q. Cui, I. A. Guzei, *J. Am. Chem. Soc*. **2005**, *127*, 14062. (b) D. A. Alonso, P. Brandt, S. J. M. Nordin, P. G. Andersson, *J. Am. Chem. Soc*. **1999**, *121*, 9580. (c) A. Comas-Vives, G. Ujaque, A. Lledos, *Organometallics*. **2007**, *26*, 4135.

25 D. V. Gutsulyak, S. F. Vyboishchikov, G. I. Nikonov, *J. Am. Chem. Soc*. **2010**, *132*, 5950.

26 (a) Z. Yan, D. G. Truhlar, *J. Phys. Chem. A*. **2008**, *112*, 6794. (b) J. Denis, A. Eric, A. Carlo, V. Rosendo, Z. Yan, D. G. Truhlar, *J. Chem. Theory. Comput.* **2010**, *6*, 2071. (c) O. N. Faza, R. Á. Rodríguez, C. S. López, *Theor. Chem. Acc*. **2011**, *128*, 647.

27 M. J. Frisch, *et. al*. Gaussian 09, Revision A.02, Gaussian, Inc., Wallingford CT, **2009.**

28 (a) P. J. Hay, W. R. Wadt, *J. Chem. Phys*. **1985**, *82*, 299. (b) W. R. Wadt, P. J. Hay, *J. Chem. Phys*. **1985**, *82*, 284. (c) A. W. Ehlers, M. Böhme, S. Dapprich, A. Gobbi, A. Hoöllwarth, V Jonas, K. F. Koöhler, R. Stegmenn, G. Frenking, *Chem. Phys. Lett.* **1993**, *208*, 111.

29 A. Hoöllwarth, M. Boöhme, S. Dapprich, A. W. Ehlers, A. Gobbi, V. Jonas, K. F. Koöhler, R. Stegmenn, A. Veldkamp, G. Frenking, *Chem. Phys. Lett*. **1993**, *208*, 237.

30 For Mo atom, the triple-ζ SDD basis set with Stuttgart-Dresden ECP was also employed, the results show that the dependence on the basis set insignificant, shown in the Supporting Information.

31 A. V. Marenich, C. J. Cramer, D. G. Truhlar, *J. Chem. Phys. B.* **2009**, *113*, 6378.

32 F. Weigend, R. Ahlrichs, *Phys. Chem. Chem. Phys*. **2005**, *7*, 3297.

33 CYLview, 1.0b; C. Y. Legault, Université de Sherbrooke, **2009**. (http://www.cylview.org).

34 The Gibbs free energy of intermediate **8** lies 2.0 kcal/mol below **TS8** at M06(6-311G(d,p)+LanL2dz) level of calculation. Employing the larger basis sets (cc-QVZP+6-311++G(2d,p), the the Gibbs free energy of intermediate **8** is calculated to be 0.8 kcal/mol higher than the transition state **TS8**. Furthermore, on the solvated E scale, the **TS8** is 2.9 kcal/mol higher than the intermediate **8** at M06(cc-QVZP+6-311++G(2d,p) level.

